Trajectory Scaling Functions at the Onset of Chaos: Experimental Results

Andrew L. Belmonte, Michael J. Vinson, James A. Glazier, Gemunu H. Gunaratne, and Brian G. Kenny[a]
The James Franck Institute, The University of Chicago, Chicago, Illinois 60637
(Received 15 March 1988)

We use an averaging technique to estimate the periodic points for attractors near the transition to chaos via period doubling and quasiperiodicity in two experimental systems. Using the averaged experimental data we then evaluate the trajectory scaling functions for both routes to chaos.

PACS numbers: 47.20.Tg, 03.40.Gc, 05.45.+b, 47.20.Ky

The universality of several simple transitions to chaos has been characterized by scaling indices,[1,2] singularity $[f(\alpha)]$ spectra,[3] and trajectory scaling functions (TSF's).[4,5] The first two methods have some disadvantages. The scaling indices determine the local behavior near at most a few points on the attractor, and contain no global information. The spectrum of singularities contains global information about the averaged orbit, but no local positional and dynamical information. The TSF, on the other hand, contains all local scaling information and also describes the global structure, so that it yields the most information about experimental transitions to chaos. However, unlike the $f(\alpha)$ spectrum,[6] the TSF depends on ratios between small nearest-neighbor distances, making it sensitive to noise. This sensitivity has been the primary obstacle to our obtaining TSF's from experimental data. In this Letter we show that we can reduce the effect of noise in experimental data by averaging. We use this technique to obtain the TSF for data from two experiments, one an electronic circuit which period doubles to chaos, and the other, a Rayleigh-Bénard system which becomes chaotic via both period doubling and quasiperiodicity.

The electronic system that we have studied is the driven diode resonator circuit,[7] consisting of two resonators in parallel, coupled by a common resistance (R_c). The current through the resonators can exhibit chaotic behavior.[8] The resonator itself (see Fig. 1) consists of a rectifier diode (1N5625), a 150-mH inductor (L), and a 1.5-Ω resistor (R_0) in series. A Hewlett Packard model 3352A function generator drives the resonators with a triangle wave, the amplitude (V) and frequency (f_{ext}) of which serve as the control parameters for the system. We measure the voltage drop across either resistor R_0 as a function of time, using an EG&G model 113 preamp, and digitally sampling at 262.144 kHz (f_{obs}) with a Hewlett Packard 35650 spectrum analyzer. For weak resistive coupling ($R_c \approx 30$ Ω), the system period doubles to chaos,[9] and we are able to obtain a clean 2^4-cycle attractor.

Since the forcing frequency of the system (f_{ext}) is only about a factor of 10 smaller than the sampling frequency f_{obs}, we obtain the Poincaré section from the time-series data by sine-curve interpolation. We make our Poincaré cut by choosing the set of local maxima $\{y_k\}$ of this interpolated signal. In Fig. 2 we plot the Poincaré map (y_n

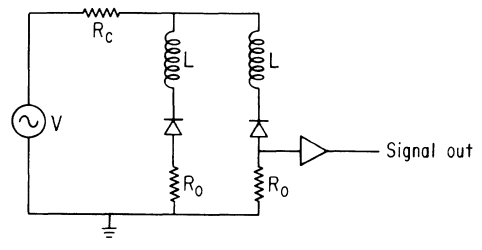

FIG. 1. The coupled driven diode resonator circuit. Each resonator consists of a rectifier diode (1N5625), a 150-mH inductor (L), and a 1.5-Ω resistor (R_0) in series. The resonators are coupled by a common resistance R_c. The circuit is driven with a forcing amplitude V, and the voltage drop is read across R_0.

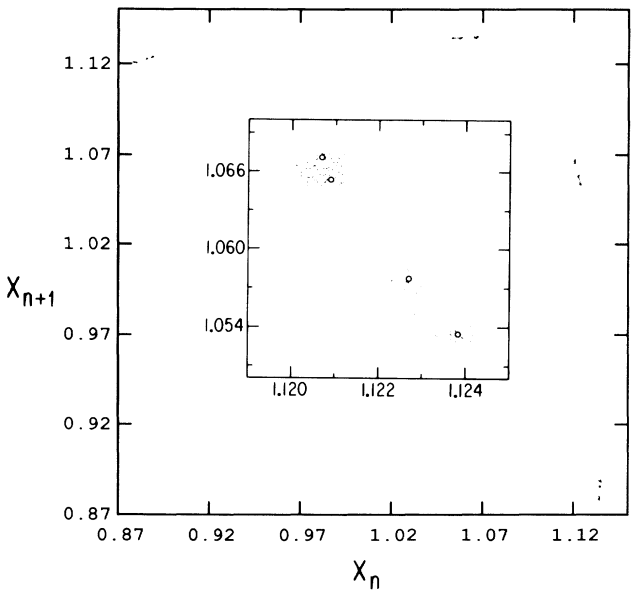

FIG. 2. The Poincaré map y_n vs y_{n+1} for the Poincaré section of extrema y_n of the experimental signal from the driven diode resonator. Note that the points are bunched into sixteen distinct domains. The noise in the data scatters the points in these regions. Inset: One group of four bunches in greater detail.

vs y_{n+1}) for a time series for which the Fourier spectrum shows a 2^4 cycle. We observe that the points of the attractor lie in sixteen disjoint regions. Since the data are noisy, these regions are diffuse, not pointlike, and we must average to estimate the positions of the actual periodic points used to calculate the TSF.

We study both period doubling and quasiperiodicity in small-aspect-ratio (two by one) forced Rayleigh-Bénard convection in mercury. We heat the fluid from below to induce the oscillatory instability (defining an internal frequency f_{int}), apply a dc magnetic field parallel to the axes of the convective rolls, and inject a pulsed alternating current to provide an adjustable perturbation (frequency f_{ext}, amplitude A_{ext}). The apparatus has been described elsewhere.[10,11] We measure the temperature oscillations at a point in the bottom of the cell and obtain a Poincaré section directly by measuring in synchronization with the external pulses. We use a bandpass filter with cutoffs at 0.01 and 10 Hz to reduce system noise. However, the dominant noise source is $1/f$ temperature drift, which cannot be effectively filtered. The internal oscillator tends to lock to a rotational ratio with the external forcing, $f_{\text{int}}=(p/q)f_{\text{ext}}$.[12,13] We tune an irrational frequency ratio by successively locking to its continued-fraction approximates, e.g., for the golden mean [$\sigma_G=(\sqrt{5}-1)/2$] we lock to the Fibonacci ratios, $\frac{2}{3}, \frac{3}{5}, \frac{5}{8}, \frac{8}{13}, \ldots$. To observe period doubling we choose a given locked tongue and increase the forcing amplitude, adjusting the frequency to find a clean period-doubling cascade.[14] As discussed in a previous paper, the two-dimensional nature of the fluid flow for strong forcing limits us to low-order bifurcations such as $2^3 \otimes \frac{8}{13}$. A complete discussion of these issues may be found elsewhere.[15]

Although the experimental attractor may be many dimensional, the dissipation is large enough so that the local structure and time ordering in both of our experimental systems appear nearly one dimensional.

We first treat the period-doubling data. Since we expect the fractal dimension of the orbit to be smaller than 1, we embed the data in three dimensions,[16] and represent each point as $\mathbf{x}_k=(x_k,x_{k+1},x_{k+2})$, where $\{x_k\}$ is the Poincaré section of the experimental time series. We define an orbit to be the time-ordered set of all nonidentical points in $\{\mathbf{x}_k\}$. Thus if we have a period-N state, the orbit is the set of points $\{\mathbf{x}_1,\mathbf{x}_2,\ldots,\mathbf{x}_N\}$, and $\mathbf{x}_{j+N}=\mathbf{x}_j$.

Let us consider what happens as we increase a control parameter through a period-doubling bifurcation to an N ($=2^n$) cycle. Just beyond the bifurcation, each point of the original orbit has split in two and the orbit does not quite close after $N/2$ points, but returns exactly after N points. Barring accidental crossings of the orbit, for any period-N orbit, $\mathbf{x}_{j+N/2}$ and $\mathbf{x}_j$ are nearest neighbors (both points having bifurcated from the same parent point). Similarly, $\mathbf{x}_{j\pm N/4}$ are the next-nearest neighbors to $\mathbf{x}_j$, having bifurcated from the parent point of $\mathbf{x}_j$.

Drift in the control parameter and other sources of experimental noise prevent us from obtaining cycles with multiplicity greater than 2^4; hence we cannot compute the limiting scalings from the 2^∞ cycle, as suggested by Feigenbaum.[4] Neither can we compare attractors with different orders of bifurcation, since we cannot measure Lyapunov exponents in real time and hence cannot obtain different attractors of the same stability. Instead, we extract the TSF by examining the hierarchy of distances within a single period-doubled attractor. For an n-fold orbit (where $N=2^n$), we define the TSF σ_j (Ref. 4):

$$\sigma_j=\begin{cases}\dfrac{\mathbf{x}_j-\mathbf{x}_{j+N/4}}{\mathbf{x}_j-\mathbf{x}_{j+N/2}}, & \text{if } 0<j\le N/4,\\[2ex] \dfrac{\mathbf{x}_j-\mathbf{x}_{j-N/4}}{\mathbf{x}_j-\mathbf{x}_{j+N/2}}, & \text{if } N/4<j\le N/2.\end{cases} \tag{1}$$

We can simplify this function by noting that iteration magnifies the effective dissipation of the map

$$T:\mathbf{x}_k\rightarrow\mathbf{x}_{k+1}, \tag{2}$$

so that high iterates are locally one dimensional.[17] Hence for large N, the points $\mathbf{x}_k$, $\mathbf{x}_{k+N/2}$, and $\mathbf{x}_{k\pm N/4}$ are nearly collinear, and σ_j reduces to a scalar function of j depending only on the absolute values of the respective distances,

$$\sigma_j=\frac{|\mathbf{x}_j-\mathbf{x}_{j\pm N/4}|}{|\mathbf{x}_j-\mathbf{x}_{j+N/2}|}. \tag{3}$$

When the map T is a diffeomorphism, σ_{j+1} and σ_j are identical to lowest order, since

$$\sigma_{j+1}=\frac{|\mathbf{x}_{j+1}-\mathbf{x}_{j+1+N/4}|}{|\mathbf{x}_{j+1}-\mathbf{x}_{j+1\pm N/2}|}=\frac{|T(\mathbf{x}_j)-T(\mathbf{x}_{j+N/4})|}{|T(\mathbf{x}_j)-T(\mathbf{x}_{j\pm N/2})|},$$

which after a first-order Taylor expansion of $T(\mathbf{x})$ about $\mathbf{x}_j$ gives

$$\sigma_{j+1}\approx\sigma_j. \tag{4}$$

The universality of σ_j follows that of the period-doubling fixed point. We show the numerically determined TSF for the logistic map in Fig. 3 (solid line) which converges after several bifurcations (~ 7). Note that the size of the steps of the TSF depends on the stability of the orbit. Figure 3 corresponds to a superstable orbit. By Eq. (4) we can extend the TSF to the continuum by defining $\sigma(x)$ on the interval $[0,\frac{1}{2}]$ as

$$\sigma(x)=\sigma_j \quad \text{for } j/N<x<(j+1)/N. \tag{5}$$

This $\sigma(x)$ is piecewise constant, with discontinuities at rational $x=n/2^m$ for n odd, the size of the discontinuity decreasing in magnitude geometrically with increasing

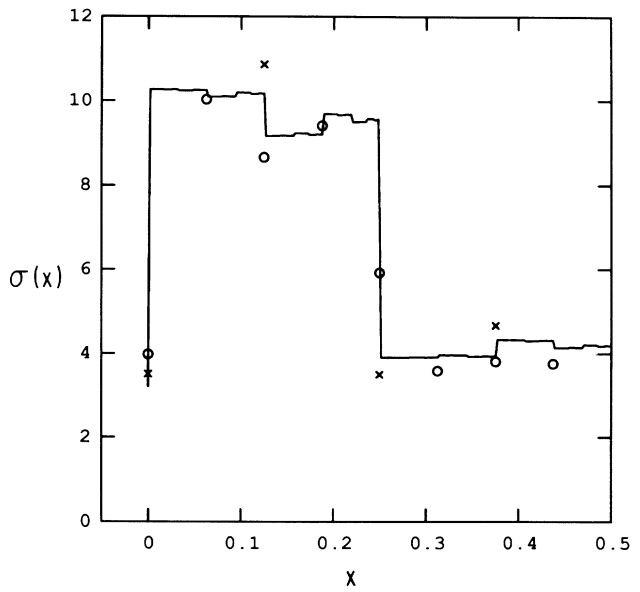

FIG. 3. The trajectory scaling function determined from the experiments (circles for the diode resonator, crosses for the Rayleigh-Bénard system) and numerically (solid line). The fluctuations of the experimental points are comparable with those for the 2^4 cycle obtained from the logistic map.

m. The lowest-order approximation to the TSF for period doubling is

$$\sigma(x)=\begin{cases}\alpha\sigma(0), & 0<x<\frac{1}{4},\\ \sigma(0), & \frac{1}{4}<x<\frac{1}{2},\end{cases} \tag{6}$$

where $\sigma(0)=3.909\ldots$ and $\alpha=2.501\ldots$ is the rescaling factor of the period-doubling renormalization group. Thus the ratio of the averages of the first and last half of the TSF will be an estimate for the rescaling factor.

If $\sigma(x)$ is known, the first $N/2$ points of the orbit determine the rest by Eq. (1). In this sense the TSF reconstructs the attractor.

An experimental time series is nearly an M cycle if it makes close return after M points. If we embed in enough dimensions, the converse is true as well: Any close return lies near an exact periodic point of the underlying iterated map (i.e., there are no accidental crossings). We exploit this result to reduce the noise in the experimental signal.[18] For fixed ϵ (typically 10^{-3}–10^{-2} times the signal amplitude) we collect those points $\mathbf{x}_t$ such that $|\mathbf{x}_{M+t}-\mathbf{x}_t|<\epsilon$. The points bunch into discrete domains of diameter η (typically 2ϵ), each corresponding to a periodic point which we locate at the center of the bunch. This averaging also reduces the effective noise by approximately $\sqrt{N_b}$, where N_b is the number of points in the bunch. We denote the periodic points by the circles in Fig. 2. An experimental signal will generally have higher-order multifurcations in addition to the 2^n cycle, e.g., $K\otimes 2^n$. In this case we estimate the 2^n cycle by averaging over $y_t, y_{t+K}, \ldots, y_{t+15K}$ within the bunches.

We determine eigenvalues of the periodic cycles by studying the evolution of the bunch of points corresponding to a point on the cycle.[18] The noise is lowest for experimental signals with small largest eigenvalues. The results presented here were taken from orbits with largest eigenvalues between -0.15 and 0.15 which correspond to superstable orbits of the logistic map.

In Fig. 3 we denote the values $\sigma(x)$ obtained from the diode experiment (averaged over several different runs) by circles, and the corresponding values from the $2^3\otimes\frac{8}{13}$ cycle for the Rayleigh-Bénard experiment by crosses. The agreement with the theoretical TSF is good. Most of the discrepancy between theory and experiment is due to the incomplete convergence of the TSF at third and fourth order which results in deviations in the theoretical values comparable to those seen in the experimental signal.

We define the rescaling factor for period doubling, α, to be the ratio between the averages of the first and second halves of the TSF. The value we obtain from the experimental data is 2.52 ± 0.05 which compares well with theoretical values of $2.501\ldots$.

Next we analyze data from the Rayleigh-Bénard system near the transition to chaos via quasiperiodicity at the golden mean.[10,19] Recall that the golden mean is approximated by the Fibonacci ratios F_{n-1}/F_n (where F_n is the nth Fibonacci number). We study periodic orbits with winding numbers close to σ_G, in this case the orbits of length F_n. As in the period-doubling case, x_i, and $x_{i+F_{n-1}}$ are nearest neighbors, and x_i and $x_{i+F_{n-2}}$, next nearest. We define the TSF for the F_n cycle to be[19]

$$\sigma_j=\begin{cases}\dfrac{|\mathbf{x}_j-\mathbf{x}_{j+F_{n-2}}|}{|\mathbf{x}_j-\mathbf{x}_{j+F_{n-1}}|}, & \text{if } 0<j\le F_{n-2},\\ \dfrac{|\mathbf{x}_j-\mathbf{x}_{j+F_{n-2}}|}{|\mathbf{x}_j-\mathbf{x}_{j-F_{n-2}}|}, & \text{if } F_{n-2}<j\le F_{n-1}.\end{cases} \tag{7}$$

We present the σ_j obtained numerically for a one-dimensional (critical) circle map. As in the period-doubling case, σ_j and the first F_{n-1} data points determine the rest of the attractor. The TSF is piecewise constant and has discontinuities at values of j with a finite continued-fraction expansion, $\langle 1,1,\ldots,1,0,0,\ldots\rangle$, the size of the discontinuities decreasing geometrically with the number of nonzero terms retained in the expansion. The discontinuities are larger than the corresponding ones for period doubling because the rescaling factor α is smaller. We extend the TSF to the continuum as before.

We denote the TSF evaluated from an experimental $\frac{13}{21}$ cycle (averaged over several data sets) by circles in Fig. 4. We find reasonable agreement with the analogous curve for the sine circle map.

The chief information that we want to extract from an

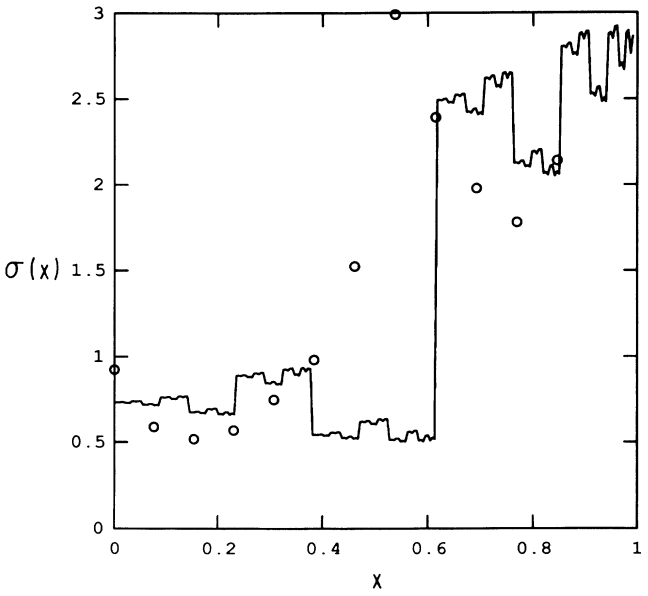

FIG. 4. The trajectory scaling function for a $\frac{13}{21}$ cycle from the Rayleigh-Bénard experiment (circles) compared with the numerical result (solid line).

experimental data set is an unambiguous identification of its universality class. In experimental systems with many degrees of freedom, this identification is difficult; hence we wish to check the details of the transition in the most thorough way possible. We believe that the TSF contains the most complete compact encoding of the universal behavior of the transition.[6] However, because of its sensitivity to noise, it is hard to determine the TSF from experimental data. Nonetheless, we can calculate the TSF by defining it correctly and by averaging the experimental data to reduce the effects of noise.

We are currently analyzing time series from intermittent and strongly chaotic data sets from the Rayleigh-Bénard experiment.[20] However, instead of examining the entire attractor[21,22] we intend to determine only the periodic points (which in this case are unstable) and their eigenvalues, since these points contain all invariant properties of the dynamical system.

We thank Leo Kadanoff and Albert Libchaber for their support of this project. This work was partially funded by National Science Foundation Grant No. DMR-83-16204 and by Materials Research Laboratory (The University of Chicago) Grant No. 8519460.

[a]Permanent address: The University of Western Australia, Perth, Australia.

[1]M. J. Feigenbaum, J. Stat. Phys. **19**, 25 (1978).

[2]S. J. Shenker, Physica (Amsterdam) **5D**, 405 (1982).

[3]T. Halsey, M. H. Jensen, L. P. Kadanoff, I. Procaccia, and B. I. Shraiman, Phys. Rev. A **33**, 1141 (1986).

[4]M. J. Feigenbaum, Physica (Amsterdam) **7D**, 16, 39 (1983).

[5]M. J. Feigenbaum, Commun. Math. Phys. **77**, 65 (1980).

[6]M. J. Feigenbaum, M. H. Jensen, and I. Procaccia, Phys. Rev. Lett. **56**, 1503 (1986).

[7]R. Van Buskirk and C. Jeffries, Phys. Rev. A **31**, 3332 (1985).

[8]P. S. Linsay, Phys. Rev. Lett. **47**, 1349 (1981).

[9]Z. Su, R. W. Rollins, and E. R. Hunt, Phys. Rev. A **36**, 3515 (1987).

[10]J. Stavans, F. Heslot, and A. Libchaber, Phys. Rev. Lett. **55**, 596 (1985).

[11]J. Stavans, Phys. Rev. A **35**, 4314 (1987).

[12]J. A. Glazier, G. Gunaratne, and A. Libchaber, Phys. Rev. A **37**, 418 (1988).

[13]J. Stavans, S. Thomae, and A. Libchaber, in *Dimensions and Entropies in Chaotic Systems* (Springer-Verlag, New York, 1986), p. 207.

[14]J. A. Glazier, M. H. Jensen, A. Libchaber, and J. Stavans, Phys. Rev. A **34**, 1621 (1986).

[15]J. A. Glazier and A. Libchaber, to be published.

[16]S. Newhouse, D. Ruelle, and F. Takens, Commun. Math. Phys. **64**, 35 (1978).

[17]P. Collet and J. P. Eckmann, *Iterated Maps on the Interval as Dynamical Systems* (Birkhauser, Boston, 1980).

[18]M. Sano and Y. Sawada, Phys. Rev. Lett. **55**, 1082 (1985); D. Auerbach, P. Cvitanovic, J. P. Eckmann, G. H. Gunaratne, and I. Procaccia, Phys. Rev. Lett. **58**, 2387 (1987).

[19]M. J. Feigenbaum, *Dynamics of Golden Mean Rotation,* edited by F. Claro (Springer-Verlag, New York, 1984).

[20]J. A. Glazier, G. H. Gunaratne, A. Libchaber, and M. J. Vinson, unpublished.

[21]J. D. Farmer and J. J. Sidorowich, "Exploiting Chaos to Predict the Future and Reduce Noise" (to be published).

[22]E. J. Kosterlitch and J. A. Yorke, "Noise Reduction in Dynamical Systems" (to be published).